HUMAN GENE THERAPY 21:143–148 (February 2010)

DOI: 10.1089/hum.2009.126

Long-Term Luciferase Expression Monitored by Bioluminescence Imaging After Adeno-Associated Virus-Mediated Fetal Gene Delivery in Rhesus Monkeys (*Macaca mulatta*)

Alice F. Tarantal[1,2] and C. Chang I. Lee[1]

Abstract

The safety and efficiency of fetal adeno-associated virus (AAV) gene delivery in rhesus monkeys and long-term monitoring of transgene expression by bioluminescence imaging (BLI) were evaluated. Early second-trimester fetal monkeys were administered AAV2/5, AAV2/9, or AAV2/10 vector supernatant preparations expressing firefly luciferase under the control of the cytomegalovirus promoter, using an intrathoracic ($n=6$) or intramyocardial ($n=6$) approach and established ultrasound-guided techniques. Postnatal BLI was performed monthly up to 6 months postnatal age ($n=12$) and then every 3 months thereafter to monitor transgene expression up to 24 months postnatal age (27 months after gene transfer; $n=6$). All AAV serotypes showed greater than 1.0×10^9 photons/sec at all time points evaluated with limited biodistribution to nontargeted anatomical sites. The highest levels of bioluminescence (photons per second) observed were noted with AAV2/9 and AAV2/10 when the three vector constructs were compared. To correlate *in vivo* findings at the tissue level, specimens were collected from selected animals and analyzed. Three-dimensional reconstruction showed that firefly luciferase expression was consistent with imaging and morphometric measures. These findings suggest that (1) high levels of AAV-mediated firefly luciferase expression can be found after fetal AAV gene transfer and without any evidence of adverse effects; (2) the intercostal muscles, myocardium, and muscular component of the diaphragm of developing fetuses are readily transduced with AAV2/5, AAV2/9, or AAV2/10; and (3) postnatal outcomes and long-term luciferase expression can be effectively monitored by BLI in young rhesus monkeys.

Introduction

Adeno-associated virus (AAV) has been used to deliver and express transgenes safely and efficiently in a variety of tissues including the heart, lung, liver, muscle, and brain (Kessler *et al.*, 1996; Limberis and Wilson, 2006; Mori *et al.*, 2006; Pacak *et al.*, 2006). Clinical trials have also shown that AAV serotype 2 (AAV2) can deliver the gene for factor IX to hepatocytes in patients with hemophilia B and achieve therapeutic levels (Manno *et al.*, 2006). AAV2 has also been developed with the capsids from other AAV serotypes in order to target specific cell populations and to evade host immune responses (Wu *et al.*, 2007). AAV is nonpathogenic in both humans and animals and has a broad host range; it is, therefore, of interest for gene therapy applications. Limited data are available for the assessment of long-term gene expression by various recombinant AAV serotypes, using *in vivo* imaging. Advances in AAV vector development combined with molecular imaging in translational models can provide important insights into the safety and efficiency of clinically relevant gene transfer approaches, and essential information before advancing to human clinical trials.

Bioluminescence imaging (BLI) provides a method for visualizing noninvasively a variety of biological processes such as gene expression, cell trafficking, viral pathogenesis, and protein functions *in vivo* (Hutchens and Luker, 2007; Villalobos *et al.*, 2007; Korngold *et al.*, 2008). Mammalian tissues have no intrinsic bioluminescence and thus imaging results in high signal-to-noise ratios when luciferase is expressed in the presence of its substrate, typically luciferin,

[1]Center for Fetal Monkey Gene Transfer for Heart, Lung, and Blood Diseases, California National Primate Research Center, and [2]Departments of Pediatrics and Cell Biology and Human Anatomy, University of California Davis, Davis, CA 95616.

in vivo. For example, firefly luciferase produces photons ranging from 530 to 640 nm with a peak wavelength at 560 nm (Contag and Bachmann, 2002). The spectral content above 600 nm, which accounts for approximately 30% of the emission spectrum of firefly luciferase, can transmit through tissues with an approximate 10-fold loss of photon intensity for each centimeter of tissue (Sadikot and Blackwell, 2005). Light transmitted through tissues shows diffuse patterns on the body surface when imaged with a charge-coupled device (CCD) camera. Images acquired by surface-imaging methods have been shown to be highly dependent on depth and the optical properties of tissues overlaying the source signal and can provide poor spatial resolution. Several mathematical models have been developed to overcome these limitations with surface imaging and to estimate the depth of the source signal (Ntziachristos *et al.*, 2000; Contag and Bachmann, 2002; Alexandrakis *et al.*, 2005). These mathematical models have been used to reconstruct bioluminescent images in three dimensions and to provide a quantitative method for analyzing signal intensity (Chaudhari *et al.*, 2005).

BLI has been successfully used in several species including mice, rats, rabbits, and monkeys to monitor transgene expression noninvasively and longitudinally, using both viral and nonviral vectors (Moriyama *et al.*, 2004; Leppanen *et al.*, 2006; Luo *et al.*, 2006; Tarantal *et al.*, 2006). In our prior studies, we showed the safety and efficiency of lentiviral vector-mediated *in utero* gene transfer and the feasibility of using firefly luciferase to monitor transgene expression postnatally in parallel with positron emission tomography (PET) (Tarantal *et al.*, 2006). In these studies an intraperitoneal (systemic) gene transfer approach was used. In the study described here, we investigated the safety, efficiency, and long-term expression of luciferase after intrathoracic or intramyocardial gene transfer mediated by AAV2/5, AAV2/9, or AAV2/10 to fetal monkeys.

Materials and Methods

Animals

All animal procedures conformed to the requirements of the Animal Welfare Act and protocols were approved before implementation by the Institutional Animal Care and Use Committee at the University of California, Davis (Davis, CA). Normally cycling, adult female rhesus monkeys (*Macaca mulatta*) ($n = 12$) with a history of prior pregnancy were bred and identified as pregnant according to established methods (Tarantal, 2005). Pregnancy in the rhesus monkey is divided into trimesters by 55-day increments, with 0–55 days of gestation representing the first trimester, 56–110 days of gestation representing the second trimester, and 111–165 days of gestation representing the third trimester (term, 165 ± 10 days) (Tarantal and Gargosky, 1995). Activities related to animal care (diet, housing) were performed as per California National Primate Research Center standard operating procedures (Davis, CA).

Vector administration and fetal monitoring

All fetuses were sonographically assessed to confirm normal growth and development before gene transfer (Tarantal, 2005). The dams were administered ketamine hydrochloride (10 mg/kg, intramuscular) or tiletamine–zolazepam (Telazol, 5–8 mg/kg, intramuscular) for these and subsequent ultrasound examinations. On the day of gene transfer, the dams were administered Telazol intramuscularly and aseptically prepared for transabdominal ultrasound-guided fetal gene transfer (Tarantal, 2005). Approximately 100 μl of AAV2/5, AAV2/9, or AAV2/10 (1.0×10^{12} genome copies [GC]; kindly provided by the Penn Vector Core, University of Pennsylvania, Philadelphia, PA) expressing firefly luciferase under the control of the cytomegalovirus (CMV) promoter was injected into fetal monkeys intrathoracically ($n = 6$; two each AAV2/5, AAV2/9, or AAV2/10) or into the myocardium ($n = 6$; two each AAV2/5, AAV2/9, or AAV2/10), using established ultrasound-guided techniques in the early second trimester (approximately 70 days of gestation) (Tarantal *et al.*, 2005). After gene transfer, sonographic measurements of the fetal head (biparietal and occipitofrontal diameters, area, and circumference), abdomen (area and circumference), and limbs (humerus and femur lengths), in addition to gross anatomical evaluations (axial and appendicular skeleton, viscera, membranes, placenta, amniotic fluid volumes), were assessed during gestation, as previously described; all measures were compared with normative growth curves for rhesus monkey fetuses (Tarantal, 2005).

Postnatal assessments

Newborns were delivered by cesarean section at term (160 ± 2 days of gestation) according to standardized protocols (Tarantal *et al.*, 2005, 2006). Cord blood samples (12–15 ml) were collected at birth (complete blood counts [CBCs], clinical chemistry panels, serum, plasma, and peripheral blood mononuclear cells) according to established protocols, and simian Apgar scores and morphometrics (birth weight; crown–rump length; head, chest, and arm circumferences; humerus, femur, hand, and foot lengths; skinfolds) were assessed (Tarantal *et al.*, 2005). Newborns were placed in incubators postdelivery and nursery-reared up through 3 months postnatal age, using standard protocols, and then housed in a juvenile housing environment. Animals were paired with another study animal for the duration of the study. Infant health, food intake, and body weights were recorded daily in the nursery and then on a routine basis (e.g., twice monthly) according to established protocols. Blood samples (3–6 ml, dependent on age) were collected monthly from a peripheral vessel to monitor CBCs and clinical chemistry panels.

Postnatal BLI

In vivo BLI for firefly luciferase expression was performed in Telazol-sedated animals immediately after an intravenous injection of D-luciferin (100 mg/kg), monthly up to 6 months postnatal age and then every 3 months thereafter, using a Xenogen IVIS 200 imaging system with Living Image software (Caliper Life Sciences, Hopkinton, MA). Each animal was placed in a light-tight chamber (0.5–10 sec) and whole body images were obtained (four views: ventral–dorsal, dorsal–ventral, right lateral, and left lateral) with quantification performed at each imaging session. Animals ($n = 6$) that received the AAV serotypes via the intramyocardial route of administration were imaged up to 6 months postnatal age, with the final imaging session on the day of tissue

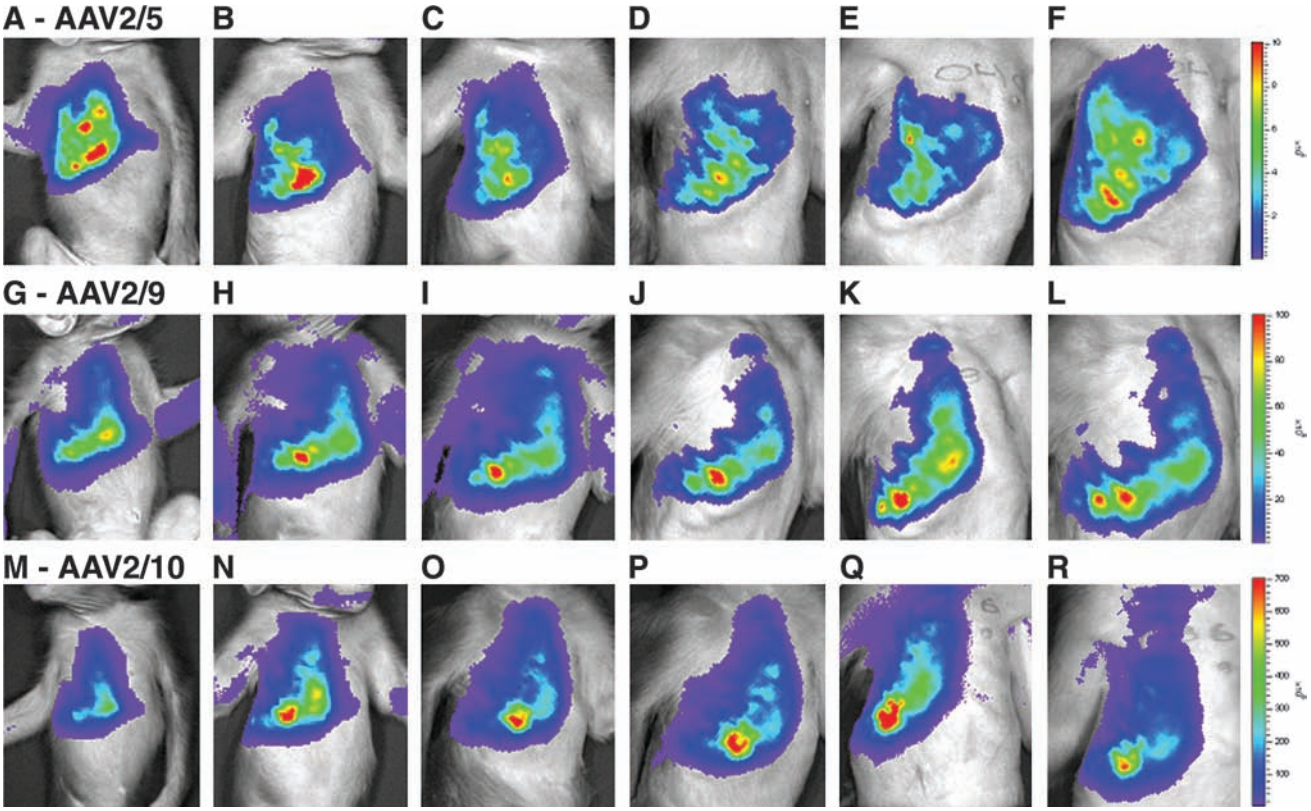

FIG. 1. Postnatal bioluminescence imaging (BLI) after prenatal adeno-associated virus (AAV) administration. Fetal rhesus monkeys were administered AAV2/5 (**A–F**), AAV2/9 (**G–L**), or AAV2/10 (**M–R**) by an intrathoracic ultrasound-guided approach. Three animals are shown (one per group) that were imaged with the Xenogen IVIS 200 imaging system after injecting D-luciferin intravenously (100 mg/kg) at 1 month: (**A**) (1.2×10^9 photons/sec), (**G**) (7.2×10^9 photons/sec), and (**M**) (2.4×10^{10} photons/sec); 3 months: (**B**) (1.0×10^9 photons/sec), (**H**) (1.9×10^{10} photons/sec), and (**N**) (7.0×10^{10} photons/sec), 6 months: (**C**) (1.0×10^9 photons/sec), (**I**) (1.4×10^{10} photons/sec), and (**O**) (5.9×10^{10} photons/sec); 12 months: (**D**) (1.5×10^9 photons/sec), (**J**) (1.5×10^{10} photons/sec), and (**P**) (5.6×10^{10} photons/sec), 18 months: (**E**) (2.2×10^9 photons/sec), (**K**) (1.6×10^{10} photons/sec), and (**Q**) (9.2×10^{10} photons/sec), and 24 months: (**F**) (2.7×10^9 photons/sec), (**L**) (1.7×10^{10} photons/sec), and (**R**) (5.0×10^{10} photons/sec). Injections were performed in the right thorax; imaging indicates no evidence of biodistribution to other anatomical sites.

harvest (6 months postnatal age). Animals ($n=6$) that received the AAV serotypes via the intrathoracic route of administration were imaged up to 24 months postnatal age (to date). Bioluminescent and photographic images were superimposed, using Living Image 2.50 software (Xenogen). Regions of interest (ROIs) were defined by selecting focal areas of bioluminescence. Total photons/sec/cm^2 (photons/sec) detected in ROIs were recorded and compared between different animals and time points. For three-dimensional imaging, multispectral bioluminescent images were obtained at 560, 580, 600, and 620 nm. These images used the surface topography and diffuse luminescence imaging tomography (DLIT) algorithm, which is a component of the imaging system (Living Image 3D analysis; Xenogen). The system uses models of photon transport in tissue to localize and quantify photon sources, and then stitches the images obtained at different views together for the three-dimensional result.

Tissue harvest

As noted previously, animals administered the AAV serotypes via the intramyocardial route were administered D-luciferin and imaged as described. The depths of anatomic locations presumed to reflect luciferase expression by BLI from the body surface were also measured sonographically with internal calipers for the ultrasound imaging system (Philips HDI 5000 SonoCT; Philips Healthcare, Andover, MA). Animals were euthanized with an overdose of pentobarbital and tissue harvests were performed according to established protocols (Tarantal *et al.*, 2005). The thickness of the skin and thoracic area was measured via ultrasound and *in situ*, and these measurements were used to assess the degree of attenuation and the accuracy of the three-dimensional reconstructions. Tissues were fixed in 10% buffered formalin and then embedded, sectioned (5–6 μm), and stained with hematoxylin and eosin (H&E) for routine histopathology.

Results

Outcome

To investigate the feasibility of using bioluminescence to monitor and assess the biodistribution of transgene expression mediated by AAV2/5, AAV2/9, or AAV2/10 noninvasively and in real time, early second-trimester fetal

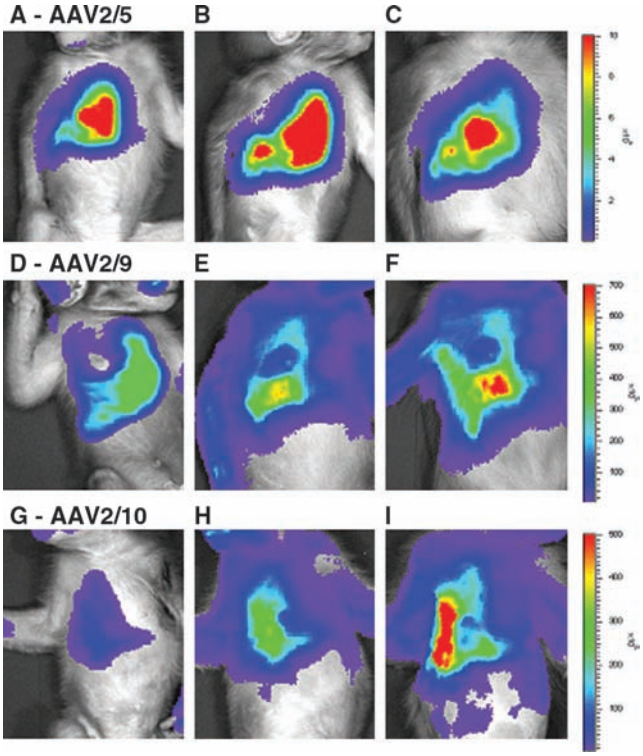

FIG. 2. Postnatal BLI after prenatal intramyocardial AAV administration. Animals administered AAV2/5 (**A–C**), AAV2/9 (**D–F**), and AAV2/10 (**G–I**) are shown at 1 month: (**A**) (1.3×10^9 photons/sec), (**D**) (8.3×10^{10} photons/sec), and (**G**) (3.5×10^9 photons/sec), 3 months: (**B**) (2.6×10^9 photons/sec), (**E**) (1.8×10^{11} photons/sec), and (**H**) (6.5×10^9 photons/sec), and 6 months: (**C**) (3.3×10^9 photons/sec), (**F**) (2.1×10^{11} photons/sec), and (**I**) (1.1×10^{10} photons/sec) postnatal age.

monkeys were administered AAV supernatant preparations expressing firefly luciferase under the control of the CMV promoter. All prenatal sonographic measures and postnatal assessments of growth and development, including CBCs and clinical chemistry panels, were within normal limits when compared with age-matched and historical controls (data not shown).

Postnatal BLI

Expression of firefly luciferase was monitored with the Xenogen IVIS 200 imaging system after an intravenous injection of D-luciferin. All animals administered the AAV vector constructs via the intrathoracic approach showed high levels of firefly luciferase expression, which was restricted to the thorax of animals administered AAV2/5 (Fig. 1A–F; range, 1.0×10^9 to 9.6×10^9 photons/sec), AAV2/9 (Fig. 1G–L; range, 7.2×10^9 to 2.7×10^{10} photons/sec), and AAV2/10 (Fig. 1M–R; range, 2.0×10^{10} to 9.2×10^{10} photons/sec). No significant differences in the level of transgene expression at all time points evaluated were observed when all animals in all groups were compared.

Infants that received AAV2/5, AAV2/9, or AAV2/10 via the intramyocardial route of administration prenatally also showed high levels of luciferase expression (Fig. 2). Luciferase expression appeared to increase when AAV2/9 (Fig. 2D–F; range, 1.1×10^9 to 8.3×10^{10} photons/sec) and AAV2/10 (Fig. 2G–I; range, 3.5×10^9 to 1.4×10^{11} photons/sec) were used at 3 months postnatal age. At 6 months postnatal age three-dimensional reconstructions were made, using images taken at 560, 580, 600, and 620 nm. Three-dimensional images showed firefly luciferase expression approximately 8 mm below the thoracic surface (Fig. 3A, C, and D), which was similar to measurements obtained by ultrasound imaging (Fig. 3B). In addition to the myocardium, the intercostal muscles and the muscular component of the diaphragm also showed luciferase expression, suggesting vector leak post-injection to these anatomical sites. These data obtained at the tissue level correlated well with the *in vivo* imaging data. When the levels of photons detected in the intercostal muscles were compared, an approximate 6-fold decline of signal was observed for a depth of 6 mm of tissue. Animals administered AAV2/10, but not AAV2/5 or AAV2/9, showed a low level of transgene expression in the myocardium (6.2×10^7 photons/sec) when compared with the muscular component of the diaphragm (2.7×10^8 photons/sec), and the intercostal muscles (6.7×10^9 photons/sec).

Discussion

Fetal gene transfer in the monkey model has been used to assess the safety and efficiency of lentiviral vector supernatant preparations (Jimenez *et al.*, 2005; Tarantal *et al.*, 2005, 2006). Prior *in utero* organ-targeted studies with lentiviral vectors in rhesus monkeys have shown that enhanced green fluorescent protein (EGFP) can be expressed safely and efficiently in specific organ systems without adverse effects, and with limited biodistribution to other sites (Tarantal *et al.*, 2005). Our prior *in vivo* imaging studies used semiquantitative methods to determine imaging outcomes, although some limitations of these modalities have previously been addressed including tissue attenuation of source signal and the generation of surface-weighted images (Tarantal *et al.*, 2006). The studies described here focused on correlating *in vivo* findings at the tissue level, and to determine whether there is loss of bioluminescence signals through attenuation from the body surface and overlying tissues. These studies showed good correlations and thus support the *in vivo* imaging outcomes observed.

Spectral content above 600 nm emitted from the firefly luciferase–luciferin reaction has been shown to penetrate through tissues with an approximate 10-fold loss of photon intensity for each centimeter (Sadikot and Blackwell, 2005). Similar to findings in mice (Contag *et al.*, 1995), the bioluminescence signal in monkeys is lost in the tissues intervening between the signal and the CCD camera. We have previously shown that a nearly 50-fold loss of photon intensity can occur when fibroblasts expressing luciferase are placed in a macroencapsulation device and then transplanted subcutaneously in young monkeys (Tarantal *et al.*, 2009). Signal attenuation can, therefore, result in limited information from tissues at greater depths when compared with more superficial structures. Therefore, it may be difficult to interpret bioluminescence data qualitatively and quantitatively if the signal is deep within anatomical structures, particularly in large animals. Bioluminescence tomography attempts to pro-

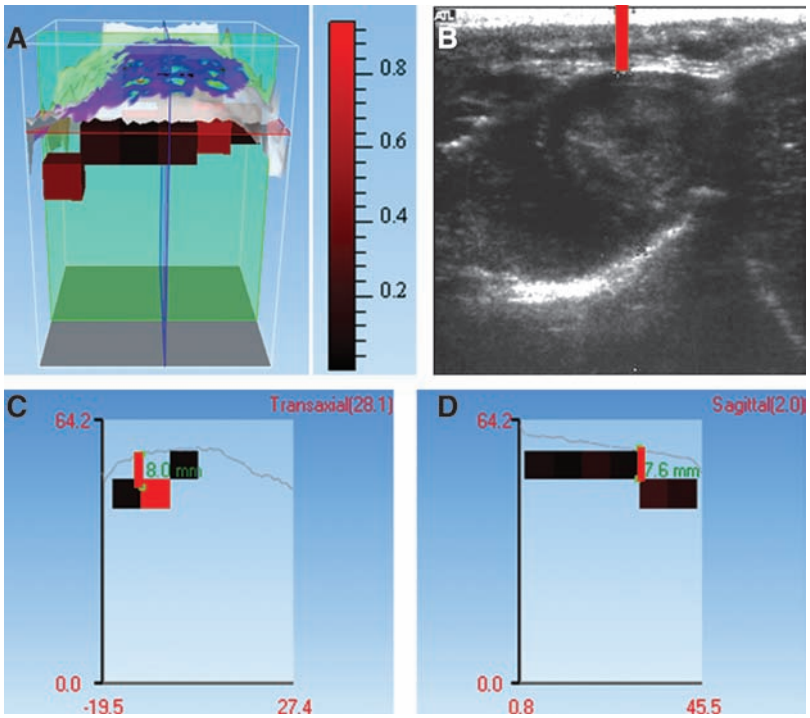

FIG. 3. Three-dimensional reconstruction of bioluminescent images. Three-dimensional reconstruction (**A**) after intramyocardial administration of AAV vector supernatant was performed, using the diffuse luminescence imaging tomography (DLIT) algorithm inherent in the IVIS 200 imaging system (scale, 10^{12} photons/sec [shown in black and red]; green plane, transaxial [**C**]; blue plane, sagittal [**D**]). The thoracic surface is represented in white. Colors on the surface represent levels of bioluminescence as shown in Fig. 2. Measurements taken from transaxial (**C**; bar, 8.0 mm) and sagittal (**D**; bar, 7.6 mm) sections were compared with measures obtained by ultrasound (**B**; bar, 6.5 mm) and showed an approximate 15% margin of error in the localization of source bioluminescence.

vide more information on the subject than surface-weighted images, as it can estimate, within some limitations, the depth and intensity of signals detected on the surface of the subject. A study on the accuracy of bioluminescence tomography reconstruction, using numerical and physical phantoms, has revealed approximately 15% error in bioluminescence intensity when compared with the actual measurements (Cong *et al.*, 2005). In the study described here, the site of firefly luciferase expression shown by bioluminescence three-dimensional tomography was consistently found within the thoracic cavity and was confirmed at the tissue level. Depending on the signal intensity at the source, it is possible that BLI may not be completely accurate for quantifying signals deeper than approximately 1.5–2 cm from the surface of young rhesus monkeys.

AAV2/5, AAV2/9, and AAV2/10 were all shown to be highly efficient in the delivery and long-term expression of firefly luciferase, with transgene expression approximately 100-fold higher than when using a dual-fusion HIV-1-derived lentiviral vector after intraperitoneal administration (Tarantal *et al.*, 2006). It is important to note that a greater quantity of infectious particles was used in the AAV study and the route of administration differed, which could account for these differences. Importantly, none of the animals administered AAV2/5, AAV2/9, or AAV2/10 showed a significant decline in the level of transgene expression, which contrasts with findings in some animals when lentiviral vectors were administered via an intrapulmonary route (Tarantal *et al.*, 2006; A.F. Tarantal, unpublished observations). Because the CMV promoter was included in these studies, silencing is not a likely explanation. The increase in luciferase expression observed in monkeys administered AAV2/9 and AAV2/10 could be related to cell proliferation with growth and maturation. It is important to note that no abnormalities or adverse events were observed in any of the animals in these studies (at present approximately 3 years after vector administration) or in other studies in which similar vector constructs were evaluated by *in vivo* imaging, and monitored for several years after fetal delivery (A.F. Tarantal, unpublished data). If sufficiently early in gestation, fetal gene transfer offers the possibility of eliminating disease as well as the potential for immune responses to transgene products and/or components of the vector(s). The long-term expression of luciferase shown in this study supports this concept, although immune responses were not directly assessed.

This study indicates the usefulness of AAV2/5, AAV2/9, and AAV2/10 in transferring and expressing high levels of luciferase under the control of the CMV promoter in rhesus monkeys, for sustained periods of time. This study further supports the use of BLI to monitor transgene expression in young nonhuman primates, to assess different vector constructs simultaneously and over time, and to provide unique insights that may not be detectable by biopsy or tissue harvest. Although there are some limitations with BLI, this technique provides an efficient and noninvasive method to monitor the expression of reporter genes *in vivo* with virtually no background noise.

Acknowledgments

The authors thank the animal care and clinical laboratory staff at the California National Primate Research Center (CNPRC) for expert technical assistance, Drs. James Wilson and Julie Johnston (Penn Vector Core) for generously providing the AAV vectors, and Dr. Simon Cherry for review of the manuscript. These studies were supported by the National Heart, Lung, and Blood Institute (NHLBI) Center for Fetal Monkey Gene Transfer for Heart, Lung, and Blood

Diseases (NIH grant HL069748) and by the Primate Center base operating grant (NIH grant RR00169).

Author Disclosure Statement

The authors have nothing to disclose.

References

Alexandrakis, G., Rannou, F.R., and Chatziioannou, A.F. (2005). Tomographic bioluminescence imaging by use of a combined optical-PET (OPET) system: A computer simulation feasibility study. Phys. Med. Biol. 50, 4225–4241.

Chaudhari, A.J., Darvas, F., Bading, J.R., Moats, R.A., Conti., P.S., Smith, D.J., Cherry, S.R., and Leay, R.M. (2005). Hyperspectral and multispectral bioluminescence optical tomography for small animal imaging. Phys. Med. Biol. 50, 5421–5441.

Cong, W., Wang, G., Kumar, D., Liu, Y., Jiang, M., Wang, L.V., Hoffman, E.A., McLennan, G., McCray, P.B., Zabner, J., and Cong, A. (2005). Practical reconstruction method for bioluminescence tomography. Opt. Soc. Am. 13, 6756–6771.

Contag, C.H., and Bachmann, M.H. (2002). Advances in *in vivo* bioluminescence imaging of gene expression. Annu. Rev. Biomed. Eng. 4, 235–260.

Contag, C.H., Contag, P.R., Mullins, J.I., Spilman, S.D., Stevenson, D.K., and Benaron, D.A. (1995). Photonic detection of bacterial pathogens in living hosts. Mol. Microbiol. 18, 593–603.

Hutchens, M., and Luker, G.D. (2007). Applications of bioluminescence imaging to the study of infectious diseases. Cell. Microbiol. 9, 2315–2322.

Jimenez, D.F., Lee C.I., O'Shea C, Kohn, D.B., and Tarantal, A.F. (2005). HIV-1-derived lentiviral vectors and fetal route of administration on transgene biodistribution and expression in rhesus monkeys. Gene Ther. 12, 821–830.

Kessler, P.D., Podsakoff, G.M., Chen, X., McQuiston, S.A., Colosi, P.C., Matelis, L.A., Kurtzman, G.J., and Byrne, B.J. (1996). Gene delivery to skeletal muscle results in sustained expression and systemic delivery of a therapeutic protein. Proc. Natl. Acad. Sci. U.S.A. 93, 14082–14087.

Korngold, E.C., Jaffer, F.A., Weissleder, R., and Sosnovik, D.E. (2008). Noninvasive imaging of apoptosis in cardiovascular disease. Heart Fail. Rev. 13, 163–173.

Leppanen, O., Bjornheden, T., Evaldsson, M., Boren, J., Wiklund, O., and Levin, M. (2006). ATP depletion in macrophages in the core of advanced rabbit atherosclerotic plaques *in vivo*. Atherosclerosis 188, 323–330.

Limberis, M.P., and Wilson, J.M. (2006). Adeno-associated virus serotype 9 vectors transduce murine alveolar and nasal epithelia and can be readministered. Proc. Natl. Acad. Sci. U.S.A. 103, 12993–12998.

Luo, J., Lin, A.H., Masliah, E., and Wyss-Coray, T. (2006). Bioluminescence imaging of Smad signaling in living mice shows correlation with excitotoxic neurodegeneration. Proc. Natl. Acad. Sci. U.S.A. 103, 18326–18331.

Manno, C.S., Pierce, G.F., Arruda, V.R., Glader, B., Ragni, M., Rasko, J.J., Ozelo, M.C., Hoots, K., Blatt, P., Konkle, B., Dake, M., Kaye, R., Razavi, M., Zajko, A., Zehnder, J., Rustagi, P.K., Nakai, H., Chew, A., Leonard, D., Wright, J.F., Lessard, R.R., Sommer, J.M., Tigges, M., Sabatino, D., Luk, A., Jiang, H., Mingozzi, F., Couto, L., Ertl, H.C., High, K.A., and Kay, M.A. (2006). Successful transduction of liver in hemophilia by AAV-Factor IX and limitations imposed by the host immune response. Nat. Med. 12, 342–347.

Mori, S., Takeuchi, T., Enomoto, Y., Kondo, K., Sato, K., Ono, F., Iwata, N., Sata, T., and Kanda, T. (2006). Biodistribution of a low dose of intravenously administered AAV-2, 10, and 11 vectors to cynomolgus monkeys. Japanese J. Infect. Dis. 59, 285–293.

Moriyama, E.H., Bisland, S.K., Lilge, L., and Wilson, B.C. (2004). Bioluminescence imaging of the response of rat gliosarcoma to ALA-PpIX-mediated photodynamic therapy. Photochem. Photobiol. 80, 242–249.

Ntziachristos, V., Yodh, A.G., Schnall, M., and Chance, B. (2000). Concurrent MRI and diffuse optical tomography of breast after indocyanine green enhancement. Proc. Natl. Acad. Sci. U.S.A. 97, 2767–2772.

Pacak, C.A., Mah, C.S., Thattaliyath, B.D., Conlon, T.J., Lewis, M.A., Cloutier, D.E., Zolotukhin, I., Tarantal, A.F., and Byrne, B.J. (2006). Recombinant adeno-associated virus serotype 9 leads to preferential cardiac transduction *in vivo*. Circ. Res. 99, e3–e9.

Sadikot, R.T., and Blackwell, T.S. (2005). Bioluminescence imaging. Proc. Am. Thorac. Soc. 2, 537–540.

Tarantal, A.F. (2005). Ultrasound imaging in rhesus (*Macaca mulatta*) and long-tailed (*Macaca fascicularis*) macaques: Reproductive and research applications. In *The Laboratory Primate*. S. Wolfe-Coote, ed. (Elsevier Academic Press, San Diego, CA) *pp*. 317–352.

Tarantal, A.F., and Gargosky, S.E. (1995). Characterization of the insulin-like growth factor (IGF) axis in the serum of maternal and fetal macaques (*Macaca fascicularis* and *Macaca mulatta*). Growth Regul. 5, 190–198.

Tarantal, A.F., McDonald, R.J., Jimenez, D.F., Lee, C.C., O'Shea, C.E., Leapley, A.C., Won, R.H., Plopper, C.G., Lutzko, C., and Kohn, D.B. (2005). Intrapulmonary and intramyocardial gene transfer in rhesus monkeys (*Macaca mulatta*): Safety and efficiency of HIV-1-derived lentiviral vectors for fetal gene delivery. Mol. Ther. 12, 87–98.

Tarantal, A.F., Lee, C.C.I., Jimenez, D.F., and Cherry, S.R. (2006). Fetal gene transfer using lentiviral vectors: *In vivo* detection of gene expression by microPET and optical imaging in fetal and infant monkeys. Hum. Gene Ther. 12, 1254–1261.

Tarantal, A.F., Lee, C.C.I., and Itkin-Ansari, P. (2009) Real-time bioluminescence imaging of macroencapsulated fibroblasts reveals allograft protection in rhesus monkeys (*Macaca mulatta*). Transplantation 88, 38–41.

Villalobos, V., Naik, S., and Piwnica-Worms, D. (2007). Current state of imaging protein–protein interactions *in vivo* with genetically encoded reporters. Annu. Rev. Biomed. Eng. 9, 321–349.

Wu, J.Q., Zhao, W.H., Li, Y., Zhu, B., and Yin, K.S. (2007). Adeno-associated virus mediated gene transfer into lung cancer cells promoting CD40 ligand-based immunotherapy. Virology 368, 309–316.

Address correspondence to:
Dr. Alice F. Tarantal
California National Primate Research Center
Pedrick and Hutchison Roads
University of California Davis
Davis, CA 95616-8542

E-mail: aftarantal@primate.ucdavis.edu

Received for publication July 20, 2009;
accepted after revision September 14, 2009.

Published online: December 30, 2009.